Atomistic Simulations of Glassy Polystyrenes with Realistic Chain Conformations

P. Robyr,*,†,‡ M. Müller,§ and U. W. Suter†

Institute of Polymers-Department of Materials, and Laboratory of Physical Chemistry, and Institute of Theoretical Computer Science-Department of Computer Science, ETH, CH-8092 Zurich, Switzerland

Received July 21, 1999
Revised Manuscript Received September 28, 1999

The detailed structure of glassy polymers is still a subject of debate. One of the main accepted views is Flory's hypothesis,[1−3] according to which the chain conformation in the glassy state is close to that in the melt or in solutions under θ conditions. However, other structural models with higher degrees of local order have been put forward (see Sperling[4] for a collection of references). Until recently, the structure of glassy polymers has mainly been studied by scattering techniques; in most studies, experimental scattering intensities are compared to those calculated from atomistically detailed chain and bulk models.[5−8] In the past few years, solid-state NMR has proven to be a powerful tool to investigate the structure of glassy solids; this technique has revealed many details about chain conformation and chain packing in glassy polymers.[9−12]

On the basis of Flory's hypothesis, Theodorou and Suter introduced an approximate algorithm to generate atomistic structures of bulk glassy polymers, known as the "amorphous-cell" method.[13] Following that work, other algorithms to generate atomistic packings of glassy polymers have been developed.[14−17] Although most of these algorithms aim at generating chain conformations close to those found in melts and specified in rotational-isomeric-state (RIS) models,[2,3] the conformations of the generated chains often depart from that target. The discrepancies are very pronounced in polymers with bulky side chains such as atactic polystyrene (a-PS).[5,8,12] Solid-state NMR measurements showed that in a-PS these large deviations from the RIS conformations are mainly artifacts of the simulations and do not occur in the bulk polymer.[12] This contribution shows that atomistic simulations of glassy polymers with conformations close to RIS models can be generated by a suitable algorithm even if the polymer chains bear bulky side groups.

To generate atomistic structures of bulk glassy polymers with periodic boundary conditions and chain conformations close to those found in RIS models, Müller et al.[18] developed a new algorithm, "PolyPack", that minimizes the nonbonded interactions within the subspace of chain conformations close to those of a given RIS model. This is in contrast to the amorphous-cell algorithm, where the conformations result from a tradeoff between the interactions due to the local conformation within a chain segment and those due to the packing of different segments.[13] Especially at the end of the chain-growing procedure used in the amorphous-cell algorithm, when the last monomer units are squeezed into the box, the interactions between different chain segments largely dominate and lead to large deviations from the RIS conformations. In this contribution, we present atomistic simulations of bulk a-PS and amorphous isotactic polystyrene (i-PS) with chain conformations close to the RIS models. These structures were generated with PolyPack and, in contrast to previous amorphous-cell simulations, agree well with solid-state NMR measurements sensitive to the chain conformation.[11,12]

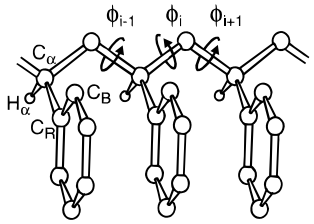

Figure 1. Meso−meso triad of polystyrene in the all-trans conformations, $\phi = 0°$. Only the hydrogen bonded to C_α is shown. The torsional angle of the side group χ:(H_α;C_α;C_R;C_B) is 0° in the three monomer units.

The generation of atomistic packings of a-PS and i-PS were performed in two stages. First, structures with chain conformations close to those of the RIS model of Yoon et al.[19] were generated with PolyPack. A structure consists of a box with periodic continuation conditions containing nine chains of degree of polymerization 40. The box edge length is 39.0 Å. In the a-PS structures, half of the dyads are meso and half racemo. The PolyPack algorithm approximates the nonbonded interactions with hard-sphere potentials only and uses fixed bond lengths and angles. Therefore, in a second stage, the structures were refined in a force field that accounts for van der Waals and electrostatic interactions and uses flexible bond lengths and bond angles. The refinement was accomplished by minimizing the energy of the structures and annealing them for 20 ps at 300 K in a molecular dynamics (MD) run with time-step increments of 1 fs. For the energy minimizations and the MD simulations, the commercial software *Discover*[20] and the unconstrained Cartesian force field pcff91[21] were used.

Further discussion of structure generation requires consideration of the RIS model. The structure of polystyrene is shown in Figure 1, with the two relevant pairs of torsional angles (ϕ_i, ϕ_{i+1}) and (ϕ_{i-1}, ϕ_i). The first column in Table 1 gives the a priori probabilities of the two pairs of angles in the two-state RIS model of a-PS by Yoon et al.[19] as a function of the tacticity. For the pair (ϕ_i, ϕ_{i+1}), only the configuration of the dyad including the two torsional angles is considered explicitly. For the pair (ϕ_{i-1}, ϕ_i), the configuration of the triad in the middle of which the two torsional angles are centered is considered explicitly. The probability matrices result from an average over the configurations of all other asymmetric carbons. The succession of the states in the matrices is trans (t) $\phi \approx 10°$, gauche (g) $\phi \approx 120°$, and gauche-bar ($\bar{g}$) $\phi \approx -120°$, as defined by the authors of the RIS model.[19]

The first step in the structure generation is to specify the target probabilities that should be reached by PolyPack. To finally reach a chain conformation close to that of the RIS model of the first column of Table 1

† Institute of Polymers.
‡ Laboratory of Physical Chemistry.
§ Institute of Theoretical Computer Science.

10.1021/ma991196u CCC: $18.00
Published on Web 11/20/1999

Table 1. Conformation Probabilities[a] of the Pairs of Successive Torsional Angles (ϕ_i, ϕ_{i+1})[b] and (ϕ_{i-1}, ϕ_i)[c] in a-PS

	RIS model of Yoon et al.[19]	POLYPACK target probabilities	POLYPACK results	POLYPACK after refinement	Amorphous cell structures[d]
$p^{r}_{i,i+1}$	0.85 0.01 0 0.01 0.13 0 0 0 0	0.84 0.01 0 0.01 0.14 0 0 0 0	0.77 0.06 0 0.06 0.11 0 0 0 0	0.60 0.11 0.01 0.12 0.15 0.00 0.00 0.00 0.00	0.28 0.15 0.08 0.13 0.19 0.04 0.07 0.05 0.01
$p^{m}_{i,i+1}$	0.06 0.47 0 0.47 0.00 0 0 0 0	0.00 0.47 0 0.47 0.06 0 0 0 0	0.01 0.48 0 0.48 0.03 0 0 0 0	0.09 0.40 0.01 0.41 0.08 0.00 0.01 0.00 0.00	0.23 0.25 0.05 0.22 0.08 0.03 0.09 0.04 0.01
$p^{rr}_{i-1,i}$	0.66 0.17 0 0.17 0.00 0 0 0 0	0.58 0.21 0 0.21 0.00 0 0 0 0	0.55 0.21 0 0.24 0.00 0 0 0 0	0.48 0.22 0.01 0.25 0.02 0.00 0.02 0.00 0.00	0.23 0.21 0.07 0.24 0.05 0.04 0.07 0.07 0.00
$p^{mm}_{i-1,i}$	0.22 0.39 0 0.39 0.00 0 0 0 0	0.16 0.42 0 0.42 0.00 0 0 0 0	0.06 0.47 0 0.47 0.00 0 0 0 0	0.13 0.40 0.01 0.41 0.04 0.00 0.01 0.00 0.00	0.20 0.25 0.07 0.28 0.06 0.06 0.04 0.04 0
$p^{rm}_{i-1,i}$	0.36 0.54 0 0.10 0.00 0 0 0 0	0.27 0.64 0 0.09 0.00 0 0 0 0	0.31 0.46 0 0.23 0.00 0 0 0 0	0.23 0.44 0.01 0.27 0.04 0.00 0.01 0.00 0.00	0.22 0.23 0.04 0.26 0.04 0.08 0.08 0.04 0.01
$p^{mr}_{i-1,i}$	0.36 0.10 0 0.54 0.00 0 0 0 0	0.27 0.09 0 0.64 0.00 0 0 0 0	0.31 0.17 0 0.51 0.02 0 0 0 0	0.20 0.25 0.00 0.51 0.03 0.00 0.00 0.00 0.00	0.21 0.24 0.07 0.25 0.07 0.06 0.05 0.05 0

[a] The succession of the states in the probability matrices is trans, gauche, and gauche-bar.[19] The probability matrices of the atomistic structures are obtained from the division of the angular domain: $-60° \le \phi < 60°$ (trans), $-60° \le \phi < 180°$ (gauche), and $-180° \le \phi < -60°$ (gauche-bar). [b] The two torsional angles (ϕ_i, ϕ_{i+1}) are those of the bonds between two asymmetric carbons with attached side chains. The corresponding dyad is either racemo (r) or meso (m). [c] The two torsional angles (ϕ_{i-1}, ϕ_i) are those of the bonds on both sides of an asymmetric carbon with an attached side chain. The configuration of the triad built by the two dyads on both sides of the asymmetric carbon appears in the superscript of the probability matrix. [d] Structures generated by Rapold et al.[5] and subsequently refined by minimizing their energy and annealing them at 300 K for 20 ps in a MD run using the force field pcff91.

and, in particular, to keep the content of meso dyads in the *tt* conformation below 10%, as required by the NMR measurements,[12] it was necessary to specify target values different from those of the RIS model because, at the beginning of the MD run, part of the meso dyads in the *tg* and *gt* states systematically tend to change to the *tt* conformation. The reasons for this trend are not clear, and the adjustment of the target probabilities was guided by the deviations of the final conformation probabilities from those of the RIS model. The target probabilities are listed in the second column of Table 1, and the probability distribution of the structures generated by PolyPack are shown in the third column. The fourth column contains the probability matrices obtained from the conformation statistics after energy minimization and MD run.

Two bulk structures of a-PS and two of i-PS were generated. The conformation probabilities aimed at and obtained for the i-PS structures were the same as those for the meso dyads and the meso−meso triads of a-PS. No conformational constraint was put on the side-chain angle χ (Figure 1) in the generation of the structures with Polypack. For both polymers, the distributions of the angle χ in the final structures is well-approximated by a Gaussian function centered at 0° with a full width at half-height of 30°.

Significant differences exist between the conformation probabilities of the RIS model aimed at and those found for the atomistic structures after refinement under the unconstrained force field pcff91. Such differences were not found when packing polyethylene.[18] They are related to the difficulty in packing polymers with bulky side groups. The largest part of the deviations arises during the structure refinement under the force field with unconstrained parameters. Notwithstanding these deviations, the probability matrices of the refined PolyPack structures are still much closer to those of the RIS model than matrices of the amorphous-cell approach, as it can be seen in Table 1. For both pairs of torsional angles (ϕ_i, ϕ_{i+1}) and (ϕ_{i-1}, ϕ_i), hardly any resemblance exists between the RIS model and the amorphous-cell structures. The differences between the conformation probabilities of the PolyPack structures and those of the structures generated with the amorphous-cell method are not due to the different box-edge lengths, b, of the simulated structures ($b = 39.0$ Å: PolyPack; $b = 18.65$ Å: amorphous-cell). Smaller PolyPack simulations with $b = 18.65$ Å and larger amorphous-cell simulations with $b = 32.0$ Å exhibit the same differences. The differences between the dyad conformation of the PolyPack structures and those generated with the amorphous-cell algorithm are illustrated in Figure 2. Whereas the

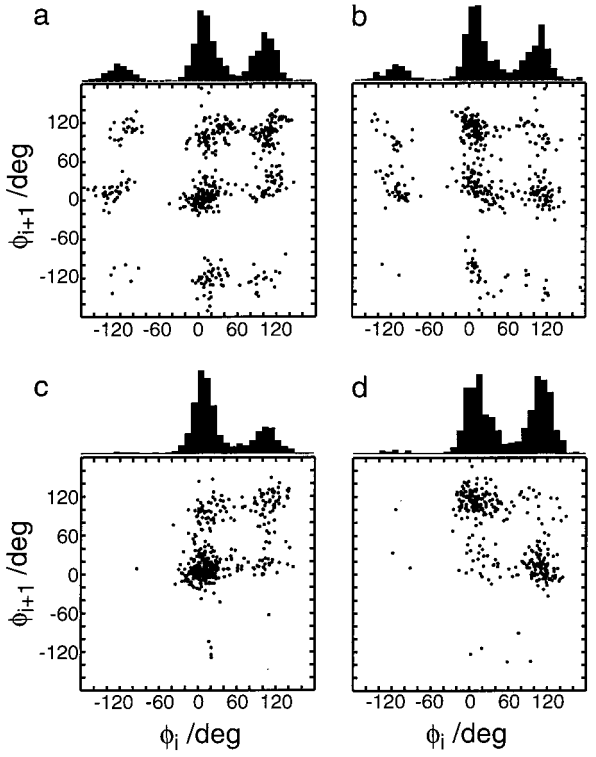

Figure 2. Torsional angles ϕ_i and ϕ_{i+1} of the meso and racemo dyads in atomistic simulations of atactic polystyrene. All of the generated structures were relaxed equally by minimizing their energy and annealing them in a 20 ps MD run at 300 K using the force field pcff91. The histograms show the overall distribution of both angles ϕ and ϕ_{i+1}. Torsional angles of the racemo (a) and meso (b) dyads of 24 atomistic structures generated with the amorphous-cell algorithm.[5,12] Each simulation box contains one chain of degree of polymerization 40. Torsional angles of the racemo (c) and the meso (d) dyads of two atomistic structures generated with the PolyPack algorithm. Each simulation box contains nine chains of degree of polymerization 40.

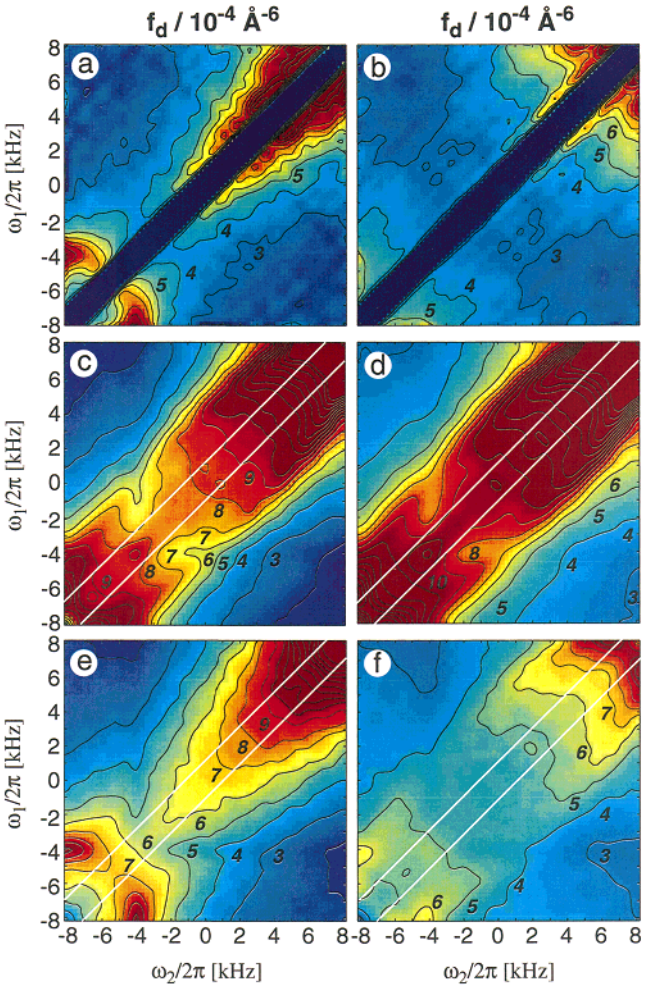

Figure 3. Distance factor f_d as a function of the resonance frequencies ω_1 and ω_2 in glassy poly(1-^{13}C-styrene). Distance factors measured by solid-state NMR in atactic (a) and isotactic (b) poly(1-^{13}C-β-^{12}C-styrene) at 298 K.[12] (c) Distance factor calculated from 24 atomistic structures of a-PS generated with the amorphous-cell algorithm.[5,12] Each simulation box contains one chain of degree of polymerization 40. (d) Distance factor of the meso dyads of the structures generated with the amorphous-cell algorithm used in part c. Distance factors calculated from two atomistic structures of a-PS (e) and two atomistic structures of i-PS (f) generated with the PolyPack algorithm. Each simulation box contains nine chains of degree of polymerization 40.

conformation distributions of the meso and the racemo dyads hardly differ in the amorphous-cell structures (Figure 2a,b), the predominance of racemo dyads in the *tt* conformation and that of meso dyads in the *tg* and *gt* conformations in the new structures are obvious (Figure 2c,d). The content of torsional angles in the trans conformation in the new structures is 61%. This value agrees with the experimental value of 68 ± 10% measured by solid-state NMR.[11]

It was shown in a previous study[12] that the distance factors, $f_d(\omega_1, \omega_2) = \langle r_{ij}^{-6} \rangle_{\omega_1,\omega_2}$, of atactic and quenched isotactic poly(1-^{13}C-styrene) are sensitive to the chain conformation; $\langle r_{ij}^{-6} \rangle_{\omega_1,\omega_2}$ is the mean of the inverse sixth power of the internuclear distance taken over all labeled spin pairs with spin i resonating at ω_1 and spin j at ω_2. The experimental distance factors measured by solid-state NMR[12] and those calculated from the atomistic simulations are shown in Figure 3. In all calculations, it is assumed that the most shielded axis z of the chemical-shielding-anisotropy (CSA) tensor of the labeled carbon is perpendicular to the phenylene plane and that the least shielded axis x is along the bond that connects the side group to the main chain (C_RC_α, Figure 1). The principal values of the CSA tensor are $\nu_{xx} = -8160$ Hz, $\nu_{yy} = -4280$ Hz, and $\nu_{zz} = -8160$ Hz, or $\delta_{xx} = 236$ ppm, $\delta_{yy} = 184$ ppm, and $\delta_{zz} = 18$ ppm from TMS.

The disagreement between the experimental distance factors (Figure 3a,b) and the factors calculated from the amorphous-cell structures (Figure 3c,d) was attributed to the large departure of the chain conformation of the simulations from those of the RIS models.[12] With this in mind, it is not surprising that the distance factors calculated from the new structures (Figure 3e,f) agree much better with the experimental data. The distance factor calculated from the new structures of a-PS (Figure 3e) well reproduces the peak at (−8, −4) kHz. This is due to the presence of a large amount of racemo dyads in the *tt* conformation (60%) together with a very low amount of racemo dyads in the $\bar{g}t$ and $t\bar{g}$ conformations (< 2%) and a low amount of meso dyads in the *tt* conformation (9%). The peak near (−8, −4) kHz and the rise at high frequencies close to the diagonal are sharper in the measured factor than in that calculated from the new structures. Because these salient features are due to racemo dyads in the *tt* conformation, this difference may indicate that the distribution of the torsional angles around the *tt* conformation is, in reality, narrower than that in Figure 2c. The distance factor calculated from

the new i-PS structures (Figure 3f) is also very similar to the measured distance factor. The low amount of dyads in the *tt* conformation (9%) together with the high content of *tg* and *gt* states (81%) in the new structures is responsible for the much lower intensity along the diagonal of the factor of Figure 3f compared to that of the factor in Figure 3d.

Overall, the distance factors calculated from the new structures are up to 20% higher than those measured by solid-state NMR. Part of this difference might still be due to inadequate chain conformation in the generated structures, although it barely exceeds the combined margins of uncertainty of simulation and experiment (ca. 15%). This difference may also be partially attributed to the static nature of the simulations, in which small amplitude motions are absent. Generally, these motions lower the distance factor or increase the distance measured by NMR between nonbonded atoms.

In conclusion, we have shown that using the new algorithm PolyPack, it is possible to generate atomistic simulations of a-PS and i-PS with chain conformations close to those specified in the RIS models, even if these polymers are difficult to pack because of the bulky side groups. Moreover, the new structures, contrary to structures generated with the amorphous-cell algorithm, are in good agreement with NMR results. This agreement supports Flory's hypothesis, according to which the chain conformation in glassy polymers is very similar to that in the melt or in solutions under θ conditions. Furthermore, if the same unperturbed chain conformations occur in the melt and in the glass, it is difficult to imagine different packings of the chain segments in the two states, as proposed in models of polymeric glasses with high degree of local order.

Acknowledgment. This work was funded by the Swiss National Science Foundation. We are very grateful to Prof. B. H. Meier and his group for their support.

References and Notes

(1) Flory, P. J. *Principles of Polymer Chemistry*; Cornell University Press: Ithaca NY, 1953.
(2) Flory, P. J. *Statistical Mechanics of Chain Molecules*, reprinted ed.; Hanser Verlag: Munich, 1989.
(3) Mattice, W. L.; Suter, U. W. *Conformational Theory of Large Molecules*; Wiley: New York, 1994.
(4) Sperling, L. H. *Introduction to Physical Polymer Science*; Wiley: New York, 1992.
(5) Rapold, R. F.; Suter, U. W.; Theodorou, D. N. *Macromol. Theory Simul.* **1994**, *3*, 19−43.
(6) Mondello, M.; Yang, H.-J.; Furaya, H.; Roe, R.-J. *Macromolecules* **1994**, *27*, 3566−3574.
(7) Furaya, H.; Mondello, M.; Yang, H.-J.; Roe, R.-J.; Erwin, R. W.: Han, C. C.; Smith, S. D. *Macromolecules* **1994**, *27*, 5674−5680.
(8) Kotelyanskii, M.; Wagner, N. J.; Paulaitis, M. E. *Macromolecules* **1996**, *29*, 8497−8506.
(9) Tomaselli, M.; Zehnder, M. M.; Robyr, P.; Grob-Pisano, C.; Ernst, R. R.; Suter, U. W. *Macromolecules* **1997**, *30*, 3579−3583.
(10) Schmidt-Rohr, K.; Hu, W.; Zumbulyadis, N. *Science* **1998**, *280*, 714−717.
(11) Dunbar, M. G.; Novak, B. M.; Schmidt-Rohr, K. *Solid State NMR* **1998**, *12*, 119−137.
(12) Robyr, P.; Gan, Z.; Suter, U. W. *Macromolecules* **1998**, *31*, 8918−8923.
(13) Theodorou, D. N.; Suter, U. W. *Macromolecules* **1985**, *18*, 1467−1478.
(14) McKechnie, J. I.; Brown, D.; Clarke, J. H. R. **1992**, *25*, 1562−1567.
(15) Borstow, W.; Kubat, J. *Phys. Rev. B* **1993**, *47*, 7659−7667.
(16) Gusev, A. A.; Zehnder, M. M.; Suter, U. W. *Macromolecules* **1994**, *100*, 615−616.
(17) Brown, D.; Clarke, J. H. R.; Okuda, M.; Yamazaki, T. *J. Chem. Phys.* **1994**, *27*, 6011−6018.
(18) Müller, M.; Nievergelt, J.; Santos, S.; Suter, U. W., submitted for publication.
(19) Yoon, D.; Sundararajan, P. R.; Flory, P. J. *Macromolecules* **1975**, *6*, 776−783.
(20) *Discover* 3.1 and *Insight* II; Biosym Technologies, Inc.: San Diego, CA, 1993.
(21) Maple, J. R.; Hwang, M.-J.; Stockfisch, T. P.; Dinur, U.; Waldman, M.; Ewig, C. S.; Hagler, A. T. *J. Comput. Chem.* **1994**, *15*, 162−182.

MA991196U